Journal of the European Ceramic Society 15 (1995) 811–821

0955-2219(95)00053-4
0955-2219/95/$9.50

Alumina of High Reliability by Centrifugal Casting

W. Huisman, T. Graule & L. J. Gauckler

Nichtmetallische Werkstoffe, ETH Zürich, Sonneggstr. 5, 8092 Zürich, Switzerland

(Received 8 September 1994; revised version received 14 February 1995; accepted 20 February 1995)

Abstract

Centrifugal casting is a powerful colloidal processing route for massive ceramic parts of high strength and high reliability. Aqueous α-alumina slurries with up to 56·8 vol.% solids content with a mean particle size of 0·46 μm were deagglomerated by ultrasonic treatment and subsequent filtration. Consolidation was performed at various centrifugal accelerations. Differential sedimentation during centrifugal casting was studied and found to be negligible for slurries with high solids loadings exceeding 50 vol.%. Green bodies with very good particle packing, showing high green densities of 68%TD (theoretical density), as well as narrow pore size distributions were obtained. High sintered densities (≥99·4%TD) with homogeneous and fine microstructures were achieved at sintering temperatures as low as 1400°C. Four-point-bending tests showed an average strength of 540 MPa with a Weibull modulus m *of 24.*

1 Introduction

Despite the outstanding properties of advanced ceramic materials, their lack of reliability still remains the highest barrier to a wider range of engineering applications.

The lack of plastic deformation in combination with flaws often up to 100 times larger than the average grain size, makes ceramic parts very susceptible to stress peaks. Thus, surface and volume flaws can lead to catastrophic failure of an entire component.[1–3] Critical flaws can be introduced via the starting powder, (e.g. impurities and hard agglomerates), during the formation of the green body (organic or inorganic inclusions, drying-induced cracks)[3,4] or during service of the component via surface damage, as well as slow crack growth.

The homogeneity of the particle packing in the green compact has a great influence on the microstructural evolution during sintering, rather than actual sintering mechanisms.[5–10] For in the case of solid state sintering, inhomogeneous (unreliable) green bodies lead to unreliable fired products. The amount and distribution of large flaws present in the green body are retained throughout the sintering process unless further flaws are introduced, e.g. due to differential shrinkage or due to exaggerated grain growth.[11] In the worst case, this can lead to an undesirably wide strength distribution in a set of ceramic components. The spread of strength values of a batch of samples is expressed by means of the Weibull Modulus m, which, for ceramic compounds (alumina, zirconia (Y-TZP), ZTA) has a value around 10, whereas metallic components show values around 100. Design engineers require values between 20 and 30.[1,2]

Hence the formation of a homogeneous, densely packed green body is one of the most important steps in the manufacturing of engineering ceramics. Average strength and reliability, especially of the low-toughness-type advanced ceramics, which obey the Griffith fracture criterion, will then be strongly increased.[12–14]

In recent years it has become evident that wet processing of powders has many advantages over dry processing in respect of reliability.

The wet processing route provides the possibility of breaking up agglomerates by milling or ultrasonic treatment or by removing them and other flaw sources from the slurry by filtration, decantation or sedimentation.

This route also allows optimal particle packing and thus a minimum in flaw size and number of flaws.[4,6,15,16] Well-known examples are slip casting, pressure filtration and electrophoretic deposition of ceramic slurries. Centrifugal casting, compared with other colloidal-forming methods, has the advantage of producing massive ceramic objects combined with a reduced risk of stress gradients in the formed part.

Stresses during the centrifugal forming process act on every volume element.[13,15,17] During sedimentation the particles move in the direction of gravity, whereas the liquid flows in the opposite

direction. This means that the total volume of liquid in the dispersion does not have to be transported through the sedimented body leaving defects such as filtration channels as in the case of slip casting and pressure filtration.

The drawback of this technology, however, is that particle size separation might occur due to differential settling during the consolidation stage.[16,18,19] There are three approaches to overcome this problem: consolidation of the system (1) in the flocculated state[18] or (2) in the coagulated state,[19] or (3) the use of highly concentrated dispersed slurries.[20] The first two approaches have been successfully used in various single-phase[18,19] and binary powder systems[19] but lead to an open structure showing bimodal porosity (intra-agglomerate: small, inter-agglomerate: large) which is undesirable for subsequent densification[5–10,21,22] because higher temperatures are needed to approach the theoretical density. It is well known that higher sintering temperatures can lead to exaggerated grain growth in the well packed regions which is equivalent to the introduction of new flaws. Several investigations severely questioned the flocculated approach by theoretically and experimentally proving an inhomogeneous density profile in centrifuged sediments from as-prepared slurries.[23–27] The third approach produced very good results for one component system with high solids loadings (≥50 vol.%).[20,28–31] Mass segregation could be avoided by hindered sedimentation in these high-solids-content slurries. Such suspensions with repulsive, nontouching particles led to green bodies with high densities and narrow pore size distributions. They show good sintering behaviour and reach high final densities at much lower sintering temperatures.[6,28–31]

The aim of the present study was to improve the mechanical properties of alumina via centrifugal casting. Of special interest for the production of such high-quality ceramic objects were the processing parameters such as solids loading, suspension conditions, sedimentation velocity and centrifugal acceleration. Green and sintered densities, sintering behaviour and microstructures were studied as well. All these results were compared to those obtained from isostatically pressed α-alumina.

2 Experimental Procedure

A commercial α-alumina powder (Ceralox HPA-0·5 with MgO, Condea, Tucson, USA) was used with a surface area of 9·4 m^2/g (BET method) and an average particle size d_{50} of 0·46 μm (d_{90} = 0·2 μm, d_{10} = 1·3 μm, Malvern Mastersizer). Chemical analysis revealed a purity of >99·97%, with the following major impurities (in ppm): Mg 293, Na 20, Si 17, Fe 13 and Ca 7, according to the supplier.

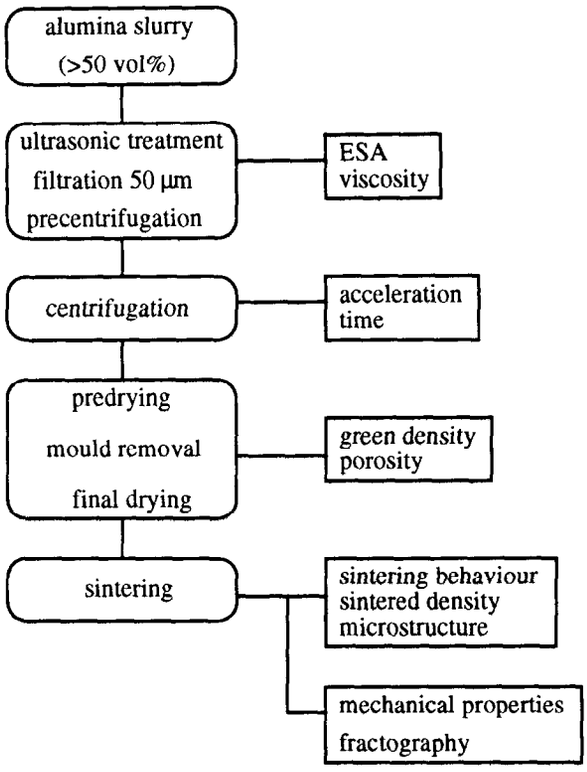

Fig. 1. Flow chart of centrifugal casting process.

Surface charge measurements were performed with 2 vol.% suspensions using an Electrokinetic Sonic Analysis System (ESA) (Matec ESA 8000, Matec Applied Science, USA). The ESA system was calibrated with Ludox TM (DuPont) 33 vol.% solids in water at a value of –3·67 mPa m/V. Viscosities of highly loaded suspensions were studied using a rotational viscosimeter (Rheomat 115A, Contraves AG, Zürich) equipped with a DIN125 testing device which varied the shear rate from 0 to 700 s^{-1} under isothermal conditions at 25°C.

The centrifugal casting process flow chart is shown in Fig. 1. Electrostatically stabilized aqueous suspensions of up to 56·8 vol.% Al_2O_3 were prepared at a pH between 4 and 4·2 using HNO_3, and subsequently dispersed by 50% pulsed ultrasonic cavitation for 8 min at 20 kHz and a power input of 420 W (Vibra Cell VC600, Sonics & Materials Inc., Danbury, USA). As the alumina used in this study is not derived by the Bayer process and therefore it is very low in Na-content, the pH did not change in between the limits given above during the subsequent preparation time. Large agglomerates, which could not be destroyed during ultrasonication, were removed by filtration (50 μm sieve) which led to slurries free of large agglomerates. These slurries were consolidated by cen-

trifugal casting (ZK 510, Berthold Hermle GmbH & Co., D-7209 Gosheim) in aluminum tubes with a diameter of 38·4 mm and a height of 110 mm. Objects with different geometries were cast in anodized aluminium moulds of which the ball-shaped one (d = 45 mm) could be disassembled into two halves along the acceleration axis. Centrifugal acceleration was varied from 150 to 4000 g to give compacts of up to 8 cm height. Centrifugation time to compact a given slurry volume of 90 cm^3 was dependent upon acceleration and ranged from 75 min to 64 h. Standard conditions were chosen, if not otherwise mentioned, with 53·4 vol.% solids content, densified at 4000 g for 90 min. Cast specimens were dried under controlled temperature and humidity conditions and then sintered in air at 1400°C with 6 h holding time. The heating and cooling rate was 1°C/min. Green and sintered densities were measured by the Archimedes principle in both mercury and water. Pore size distributions in green compacts were determined by mercury porosimetry with pressures up to 2000 bar (Hg-Porosimeter 2000, Carlo Erba Strumentazione, I-Milano). For analysis the cylindrical model was used,

Other samples using the same alumina powder were prepared by isostatic pressing at 350 MPa for 3 min. The sintering temperature for those samples was 1500°C with a 2 h holding time. The sintering behaviour in air was monitored with a differential dilatometer (Type 802, Bähr Gerätebau GmBH, D-4971, Hüllhorst), using a sapphire reference.

Bending test specimens of 4 × 3 × 45 mm (width, height, length) were cut out of a sintered cylinder in the direction of the acceleration axis. Strength measurements were performed according to the four-point-bending test method DIN 51 110 (Instron 8652, Instron Ltd., HP12 3SY, England) with 20/40 mm spans and a crosshead speed of 2 mm/min. Microstructures were observed by LM and SEM on polished and thermally etched surfaces. Mean grain sizes were obtained by measuring the intercepts of about 200 grains per sample and multiplying the average value by 1·5.[32] K_{Ic} measurements were performed in air by the Vickers indentation method (Zwick, D-7900, Ulm) using the Evans and Charles approach to evaluate fracture toughness.[33]

3 Results and Discussion

3.1 Suspension stability and viscosity

To avoid preferential segregation during centrifugal casting, highly stabilized dispersed systems with high solids content are required.[19,28–30] It is well known that the stability of suspensions increases with increasing electrokinetic sonic amplitude signal (ESA) which is directly proportional to the Zeta potential. Figure 2 shows the change in ESA signal in the pH range from 3 to 11 for an Al_2O_3 suspension containing 2 vol.% solids. The region of highest ESA signal lies around pH 4 and the isoelectric point at pH 9. Below pH 4 the solubility of Al_2O_3 increases drastically. Since the formation of dissolved Al^{3+} ions has a deteriorating effect on the sintering behaviour of alumina,[31] the plateau region around pH 4 was chosen to stabilize the suspensions.[19,28,29]

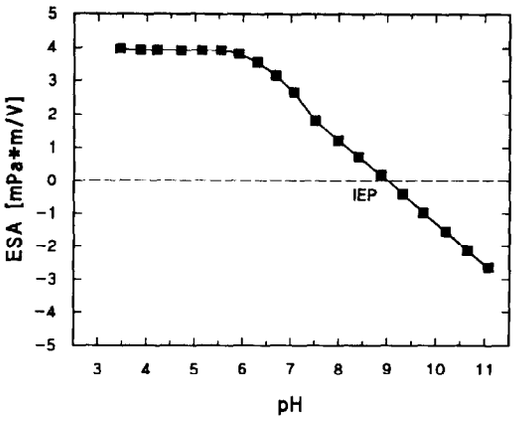

Fig. 2. ESA signal versus pH for a 2 vol.% alumina suspension.

The highest possible powder content is desirable for centrifugal casting in order to prevent separated sedimentation, but also to save space (for supernatant water) and weight (of the moulds) during the centrifugation step. On the other hand, high solids loadings are limited by the increase in viscosity (Fig. 3), and by rising pseudoplasticity. In addition, higher powder contents in the slurry result in increased losses of material during filtration and increased difficulties during mould filling.

In order to explore an optimum solids content of the suspension, slurries with 50·1, 53·4 and 56·8

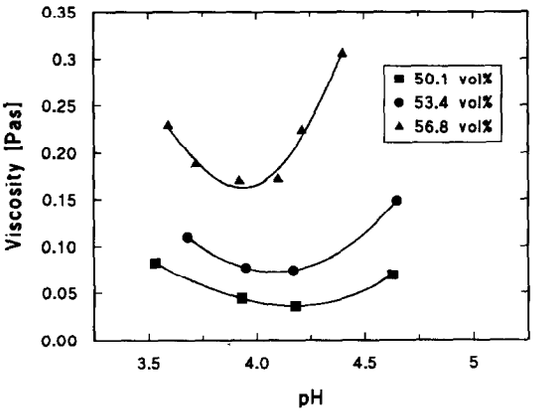

Fig. 3. Viscosity (at shear rate 100 s^{-1}) versus pH for alumina suspensions with different solids loadings.

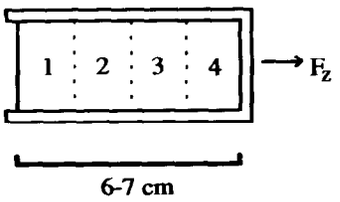

Fig. 4. Segmentation and numbering of cylindrical green compact.

vol.% solids were made at various pH values around pH 4. Figure 3 shows the viscosities at a shear rate of 100 s^{-1} (η_{100}) for slurries with different solids loadings around the optimal pH (≈ 4) found in ESA measurements. With rising powder content, the minimum of lowest viscosity will increase from 3 mPa s (50·1 vol.%, at pH 4·2) to 160 mPa s (56·8 vol.%, at pH 3·95). In addition, the viscosity/pH curve's minima shift slightly to lower pH values while narrowing considerably with augmenting powder content.

3.2 Solids content, green density and porosity

To define the limits of hindered sedimentation, slurries of different powder contents from 36·9 to 56·8 vol.% were cast in aluminum tubes at 4000 *g* for 90 min. All suspensions were stabilized at a pH between 4 and 4·2. The dried compacts were cut into segments of about 1·5 cm height to determine their green density and porosity. The numbering of the segments is shown in Fig. 4. Green densities and average pore radii (r_{50}) are summarized in Table 1.

All top segments show a green density that is lower than that of segments closer to the bottom of the cylinder. This difference is negligible for all parts that were cast from slurries with a powder content higher than 51·7 vol.%. If the solids loading was chosen below this value, a much larger deviation in green density could be measured. Obviously, differential sedimentation occurred in those slurries and finer particles were packed at the top corresponding to smaller pores found as well. Porosimetry measurements revealed a different mean pore size (Table 1), a different cumulative volume and a different surface area for top and bottom parts of compacts made from those low-

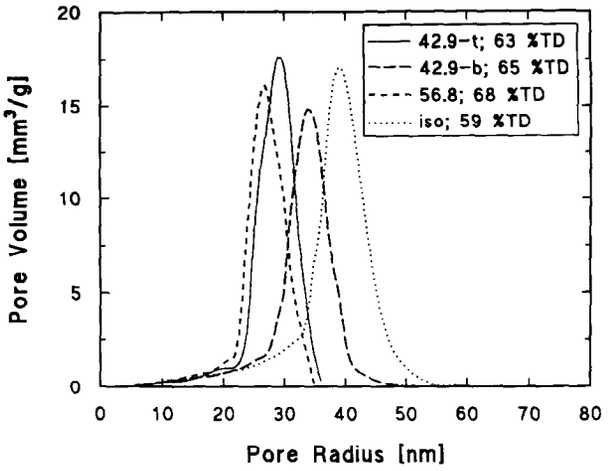

Fig. 5. Porosimetry data of 42·9 vol.%-slurry compact, 56·8 vol.% compact and isopressed compact (segments).

loaded slurries (<50 vol.% powder). It is well known, that monosized particles do pack more homogeneously but lead to lower densities (63 versus 68 %TD) than multisized powders. The change in surface area is due to the fact that larger particles pack at the bottom (smaller BET) and finer ones pack at the top (larger BET) in the case of particle size separation. As can be seen from Fig. 5, the average pore radius decreases from the bottom to the top segment of a 42·9 vol.% slurry-cylinder from 35 to 29 nm. In contrast to these findings, a 56·8 vol.% slurry-compact shows an average pore radius of 28 nm over the entire length of the cylinder, as well as a homogeneous and high green density of 68%TD. This indicates that no separation occurred during the centrifugation process. For comparison reasons, the pore size distribution of an isostatically pressed sample is also displayed. This dry processed sample (59%TD) has a broader pore size distribution than all wet processed samples and the highest average pore radius of 41 nm. Thus, the particle packing of colloidally processed samples is much better (63–68%TD) than that of an isostatically pressed sample (59%TD).

Shih *et al.*[25,27] have elaborated a theoretical approach to predict the density profiles of centrifuged cakes from flocculated suspensions by

Table 1. Green density (GD, in %TD) and average pore size (r_{50}, in nm) of segmented cylinders

Slurry (Vol.%)	*Segment 1*		*Segment 2*		*Segment 3*		*Segment 4*	
	GD	r_{50}	*GD*	r_{50}	*GD*	r_{50}	*GD*	r_{50}
36·9	62·8	27·0	64·2	30·0	66·2	33·5	66·5	39·3
42·9	63·0	27·1	63·7	33·1	64·0	36·0	66·0	34·6
50·1	64·2	27·0	65·0	28·7	66·5	28·9	66·5	29·9
51·7	65·0	27·5	65·2	29·8	68·5	28·7	67·7	28·8
53·4	65·0	29·3	65·7	30·6	66·7	30·0	66·5	30·0
56·8	67·6	27·5	68·1	28·3	68·3	28·2	68·1	27·5

implementing their experimentally obtained power-law pressure–density relationship[23] into the general differential equations for centrifugation[17] with appropriate boundary conditions. Their calculations were formulated in the equation

$$\frac{\Phi(z)}{\Phi_{max}} = \left[1 - \left(\frac{z}{z_m}\right)\right]^{\frac{1}{(n-1)}} \quad (1)$$

where $\Phi(z)$ is the volume fraction of solids at elevation z (measured from the bottom of the tube), Φ_{max} is the maximum solids volume fraction (measured at $z = 0$) and z_m is the elevation at equilibrium state. The exponent n indicates the flocculation state of a system during compaction. Generally, n decreases as the degree of flocculation increases. Their predictions agreed very well with the pronounced density profiles they measured in cakes that were centrifuged from flocculated alumina and boehmite suspensions. The uniform density profiles found in this investigation can be described by their equation as well. Green densities GD(z) instead of volume fractions $\Phi(z)$ were used for the calculations made in this study. This is, especially for the high loaded suspensions, a tolerable approximation. A linear drying shrinkage of 0·5–1·0% equals a volume reduction of 1·5–3·0%, indicating that the actual volume fraction for a green density of 0·68 would then be 0·67 or 0·66. Due to the high green densities obtained in this investigation, Φ_{max} was set to 0·685 (instead of 0·64 for random packed spheres[25,27]). Green densities of cylinders compacted from a 36·9 vol.% and a 56·8 vol.% slurry are displayed in Fig. 6. Three curves calculated according to Ref. 27 are shown as well. The n values chosen are $n = 9$ for a flocculated suspension[25,27] and $n = 100$ to fit the dispersed suspension with low (36·9 vol%) solids content. Hereby it has to be emphasized that for dilute alumina suspensions, a density gradient is

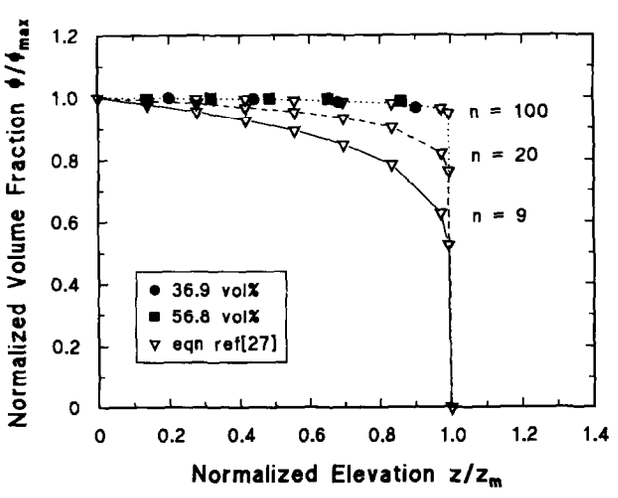

Fig. 6. $\Phi(z)\Phi_{max}$ versus z/z_{max} for green densities of compacts made from 36·9 and 56·8 vol.% slurries. Triangles are calculated values according to Ref. 27.

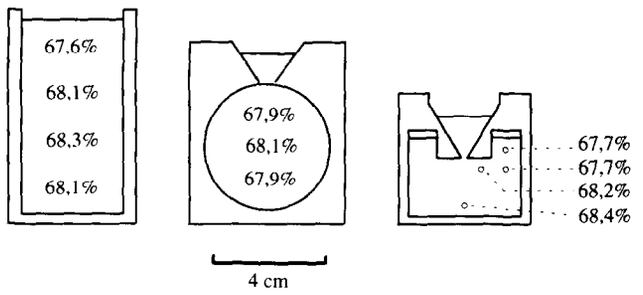

Fig. 7. Green density distribution of compacts shaped in different moulds: (a) cylinder; (b) ball; (c) with extreme constriction (53·4 vol.% slurry).

found due to particle size separation and not due to a pressure gradient in the centrifuged cylinder. For dispersed suspensions containing high volume fractions, the density–elevation relationship can be described if $n = 150$ is applied, which expresses virtually a step function and therefore a negligible density gradient.

Based on the results obtained so far, a solids loading of 53·4 vol.% was chosen for further experiments to be the best compromise between good handling of the suspensions and highest possible powder content.

During centrifugation the centrifugal force on the particles acts radially to the centre of the centrifuge. The question arises as to how a mould with undercuts can be filled properly with solids. Beylier *et al.*[20] have shown that the casting process can properly fill past constrictions in their spool and screw moulds. In order to elucidate the limits of mould filling, a mould containing an extreme undercut (Fig. 7c) was constructed. Centrifugal casting was performed with a 53·4 vol.% slurry. After centrifugation, the undercut was filled up to 65% of its height (10 mm) with alumina, leaving the upper part filled with clear water. The cast undercut was of stable shape and did not flow away after immediate removal of the top part of the mould. There was no evident difference in green density in this highest annular-shaped segment compared to the rest of the compact (Fig. 7(c)). Sintering led to a compact that showed no cracks and a homogeneous density. As can be seen from Fig. 7, high and homogeneous green densities of about 68%TD could be achieved in all moulds used throughout this investigation.

3.3 Mould-filling factor

To study dependence of the velocity of sedimentation upon the maximum applied acceleration, a slurry with 53·4 vol.% solids content was centrifuged at different accelerations for various times. The time t_{eq} to reach the equilibrium-state height z_m of a suspension by centrifugation is proportional to the initial slurry column height H_0

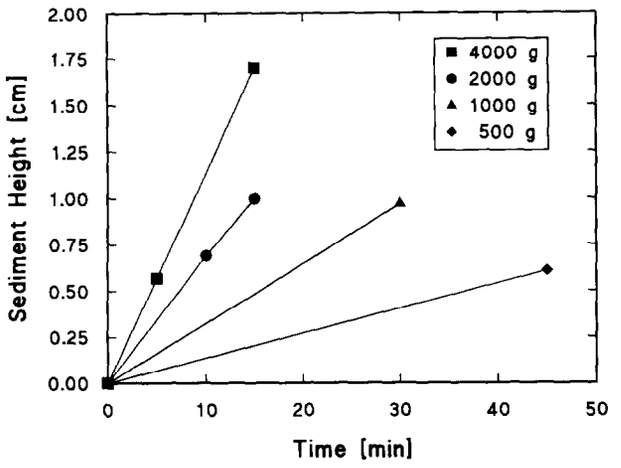

Fig. 8. Sediment height versus centrifugation time of a 53·4 vol.% slurry at various centrifugal accelerations.

and inversely proportional to the centrifugal acceleration $\omega^2 R$ where R is the radius of the centrifuge ($z = 0$).[24]

$$t_{eq} \approx H_0/\omega^2 R \quad (2)$$

At 4000 g the settling rate of the suspension in a cylindrical mould with a diameter of 38·4 mm is 0·12 cm/min, as shown in Fig. 8. To settle down the same amount of slurry and reach the same green density at 500 g, the centrifugation time is 6·6 times longer, and at 150 g, 26 times longer. No evident difference in homogeneity of the compact density was detected. After 15 min centrifugation at 4000 g the body does not show any plastic deformation under its own weight anymore. With lower solids contents, the settling rate will increase but differential sedimentation will occur due to increased inter-particle distances.

3.4 Drying and drying shrinkage

After centrifugation, the supernatant water is removed. Then the centrifuged green bodies still contain between 9 and 11 wt% water, which will evaporate during drying. It is well known that fast evaporation of the liquid during and especially at the end of the constant rate period (CRP) can lead to the formation of cracks in the green body, resulting in a low yield after sintering.[34] To detect the limits of successful, (i.e. crack-free) drying of centrifuged compacts, drying was performed while varying the parameters of temperature and relative humidity (RH). Cast compacts were dried under the following conditions: (1) in an oven at 50°C, (2) at ambient, (3) in a temperature-controlled humidity chamber at 25°C and 97%RH and (4) totally protected from direct convection at 25°C/97%RH. After casting, one-half of the ball-shaped mould was removed immediately after casting and the compacts were dried under the aforementioned conditions. The weight loss of the drying compacts was monitored over time and is displayed in Fig. 9. The final weight (dry body) was subtracted from that of the starting weight (wet body without supernatant) to give the value for the total water content in the cast compact (≡100%, Fig. 9). The fastest drying rates were achieved under oven and ambient conditions, followed by the nonconvection-protected compact under climatized conditions (25°C/97%RH) and with the slowest rate for the full convection-protected ball. As soon as drying rates are faster than 1·5% of the total water content of the green body per hour, the possibility of crack formation in the sintering body will be strongly increased. Compacts dried in the oven or under ambient conditions could not be sintered without cracking. In addition to that, it is important to protect the drying green bodies from direct convection as the CRP drying rate will be decreased with increasing layer of standing air over the compact. Normally, after a drying period of 4–5 days under climatized conditions, compacts could be sintered without cracking.

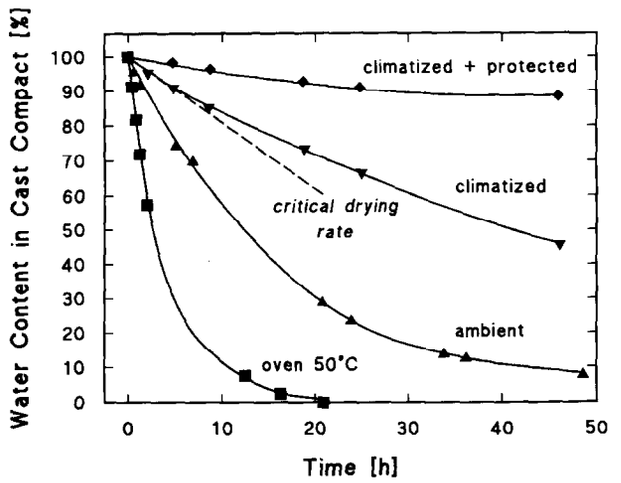

Fig. 9. Drying behaviour of ball-shaped cast compacts under various conditions.

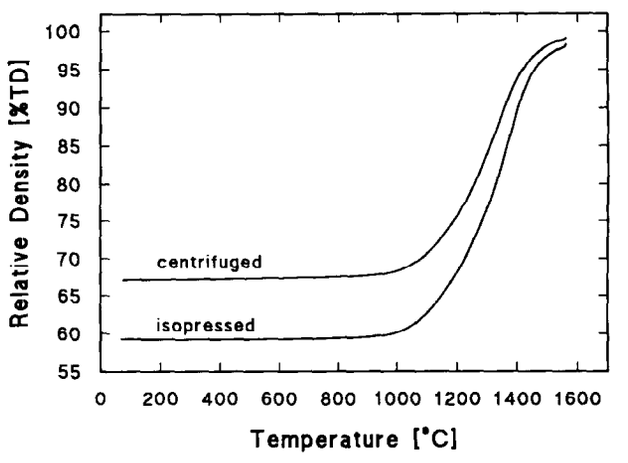

Fig. 10. Sintering curve of isopressed and cast alumina (53·4 vol.% slurry, 4000 g/90 min) at a constant heating rate of 5°C/min.

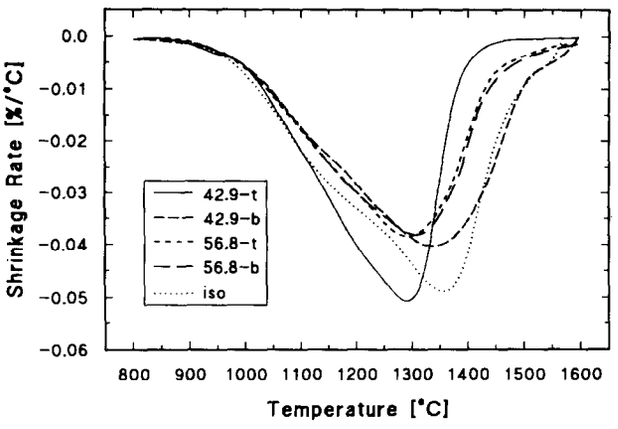

Fig. 11. Shrinkage rates of segments of cast alumina parts produced from 42·9 and 56·8 vol% slurries and of isopressed alumina.

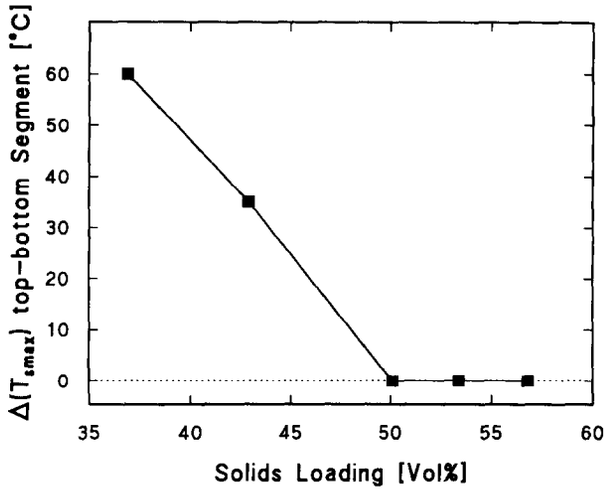

Fig. 12. Influence of solids loading on the difference of temperature of the maximum shrinkage rate $\Delta(T_{smax})$ between top and bottom segments of the centrifuged cylinders.

Linear shrinkage during drying was in the range 0·5–1·0% for compacts produced from high-solids-content slurries. This is equal to a volume reduction of 1·5–3·0% for compacts produced from high-solids-content slurries. Assuming a straight line of average-sized particles, this corresponds to an inter-particle distance of 5 nm in the sedimented wet state which is, according to the DLVO theory, just of the order of the distance of the primary minimum barrier. This calculation model, however, is very simplified and does not take into account the three-dimensional rearrangement behaviour of a drying particle system.

3.5 Sintering behaviour

The change in relative density during constant-heating-rate sintering (5°C/min) is shown in Fig. 10. The wet processed sample, which was produced from a 53·4 vol.% slurry, starts from a higher green density (68%TD) and reaches a higher final density at lower temperature than the dry processed sample (59%TD). This is due to the fact that larger pores disappear or get smaller, reaching an equilibrium size at higher temperatures and at a lower rate than small pores.[22,23] The isopressed part shows a wide pore size distribution from 0 to 60 nm around an average pore radius of 41 nm, whereas the centrifuged part has a smaller r_{50} of 29 nm and a narrow pore size distribution (Fig. 5). This proves that the finer the pores and the narrower the pore size distribution, the faster and earlier ceramic parts will sinter to maximum density.[6] Hence, centrifugal casting leads to a good sintering behaviour due to homogeneous particle packing in the case of high-solids-content slurries.

For a further illustration of the sintering kinetics, the shrinkage rates of three green compacts are compared in Fig. 11. A compact made from a relatively low solids loading slurry (42·9 vol.% Al_2O_3) showed different shrinkage rates at the top (t) and the bottom (b) of the compact. Due to differential sedimentation in this compact, the top consists of finer particles and finer pores (as illustrated in Fig. 5) than the bottom and therefore shows sintering at lower temperatures than the bottom part. This difference becomes negligible in the case of compacts made from high-solids-loading (56·8 vol.%) slurries. Both parts, top and bottom, show identical shrinkage rates over the whole sintering regime (Fig. 11). For comparison reasons, the shrinkage rate of an isostatically pressed sample is shown too. In the beginning (up to 1100°C) well-densified intra-agglomerate regions are responsible for the shrinkage, and the shrinkage rate is very similar to that of the 42·9 vol.% top segment. However, due to the larger inter-agglomerate pores, the temperature for the maximum shrinkage rate is not reached until 1375°C and the final density even at 1600°C is not as high as that of the cast compact (Fig. 10).

The findings from Fig. 11 can be illustrated in a different manner. Fig. 12 shows the influence of solids loading on the difference in temperature of the maximum shrinkage rate for the top and bottom segments of the cylindrical compacts. With rising solids loading, this temperature difference decreases from 60°C in the case of a 36·9 vol.% slurry over 35°C at 42·9 vol.% and becomes negligible for green bodies made from suspensions with solids loadings higher than 50 vol.%. This means that for a solids content above 50 vol.% no differential shrinkage over the length (8 cm) of a compact occurs. These findings agree with the results of the porosity measurements (Table 1), crack formation (Table 2) and the gradient degree in light scattering of polished cross sections (lengthways

Table 2. Density and appearance of sintered cylinders (1400°C/6 h)

Slurry (vol.%)	*Sintered density (%TD)*	*Sintered compact*
36·9	99·72	Cracks, gradient
42·9	99·50	Cracks, gradient
50·1	99·44	OK
51·7	99·47	OK
53·4	99·40	OK
56·8	99·35	OK

of centrifugation axis) of sintered cylinders produced from slurries containing less than 50 vol.% solids.

3.6 Sintered density

Table 2 shows the differences in sintered density after 6 h at 1400°C for the entire cylinders. Centrifugal casting leads to sintered densities of more than 99·3%TD which are significantly higher than those of isostatically pressed material (98·6 %TD). Highest densities were reached with cylinders made from slurries with low solids contents (36·9 and 42·9 vol.%), but, however, the particle separation led to the formation of cracks during the firing process, as well as to a gradient degree of

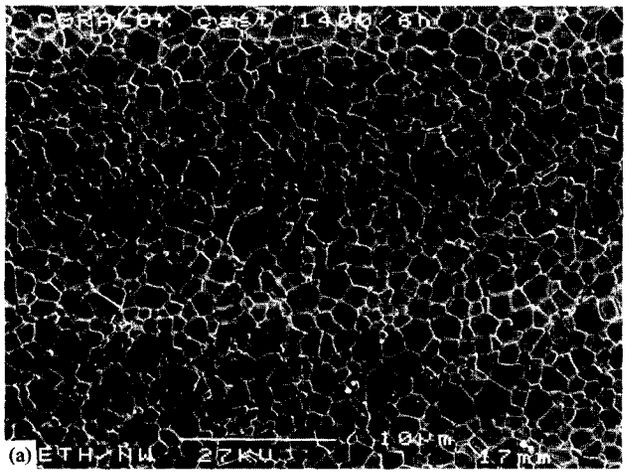

Fig. 13. Microstructures of sintered compacts: (a) centrifugally cast (53·4 vol.% slurry, 4000 *g*/90 min); (b) isostatically pressed.

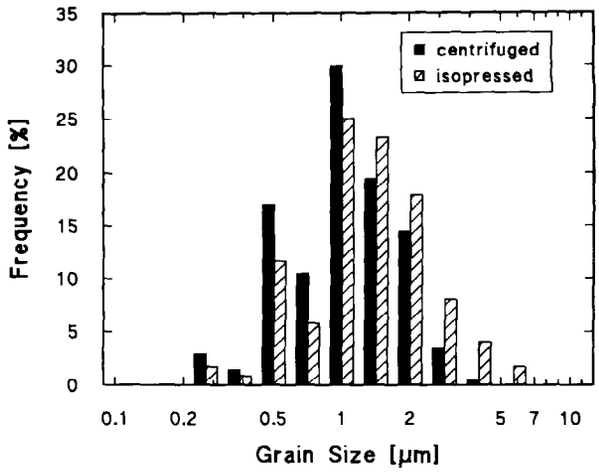

Fig. 14. Statistical evaluation of microstructures of sintered compacts.

light scattering over the length of the cylinder. This is due to the different sintering kinetics of larger and smaller particles (and larger and smaller pores) at the top and bottom part of the cylinder, respectively. Slurries containing more than 50 vol.% solids gave crack-free sintered parts that showed densities of about 99·4%TD and homogeneous light scattering throughout the entire length of a cylinder.

3.7 Microstructure

At the same final density (99·4%TD) a finer and more homogeneous microstructure is achieved by centrifugal casting compared to isopressed samples, as can be seen from Fig. 13. A statistical evaluation of the micrographs is shown in Fig. 14. The average grain size measured was 1·1 μm for the centrifuged samples and 1·6 μm for the isopressed alumina. The most important difference lies in the homogeneity of the microstructure. Isostatically pressed alumina shows grains of up to 10 μm in size, whereas the maximum grain size in cast alumina does not exceed 6 μm. Grain growth can occur in densified regions and its speed is strongly dependent upon the temperature. The lower the sintering temperature to reach a high final density, the better for the microstructural evolution which will be finer and more homogeneous.

3.8 Flaw size distribution

Figure 15 shows polished surfaces of cast and isostatically pressed alumina of comparable density (99·4%TD). By colloidal processing the number and size of larger pores could be drastically reduced. This can be more clearly seen from Fig. 16 which shows a statistical evaluation of the flaw distribution of centrifugally cast and isopressed samples. The largest pores in sintered compacts from cast alumina reach a size of 20–30 μm, which is about 4–5 times smaller than the largest

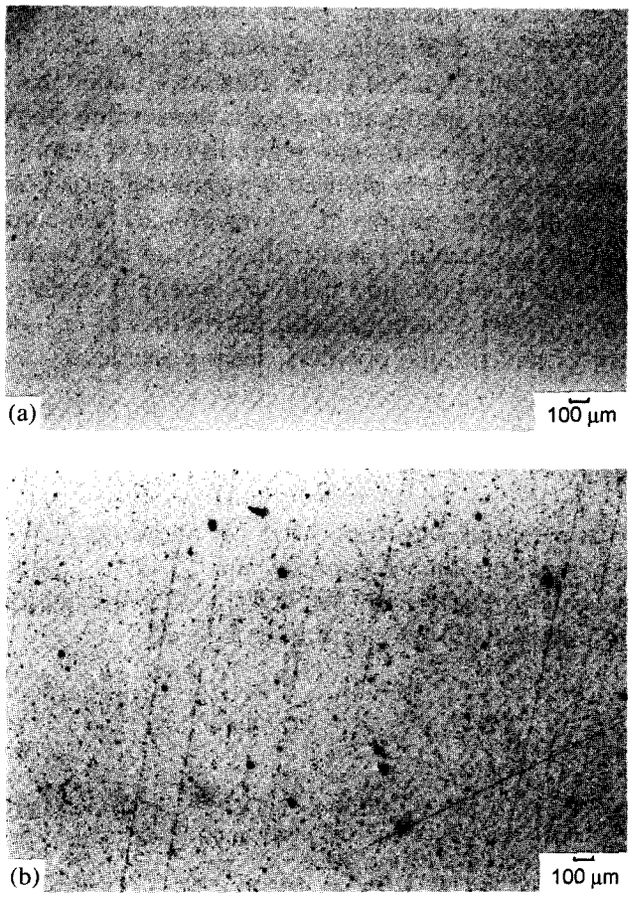

Fig. 15. Polished surfaces of sintered compacts: (a) centrifugally cast (53·4 vol.% slurry, 4000 *g*/90 min); (b) isostatically pressed.

pores found in isopressed material (90–120 μm). The area investigated on both samples was 5·6 mm^2. The total pore volume equals 5 ppm of the total volume.

Fracture surfaces of centrifuged bending test specimens were examined with SEM (Fig. 17) and the fracture origins were recognized to be agglomerates having a size of 20–30 μm. This is typical for the maximum flaw size of the centrifuged compacts of this study and is in accordance with the Griffith relationship for the case of a fracture

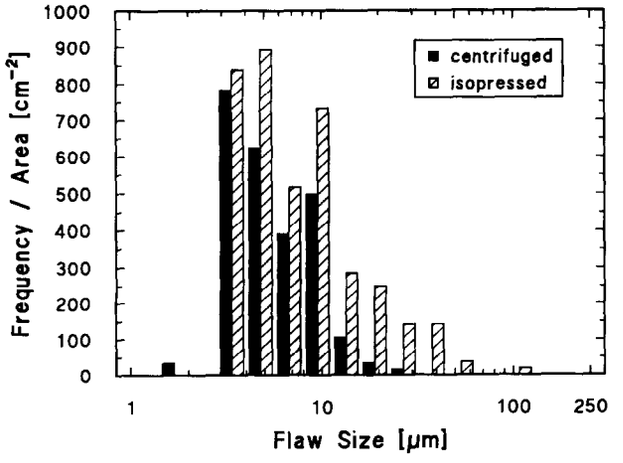

Fig. 16. Statistics of flaw distribution in sintered compacts.

Fig. 17. Typical fracture surface of centrifuged bending test specimen showing the fracture origin.

toughness of 3·8 MPa $\sqrt{m}$ and an average bend strength of 540 MPa, (geometry factor Y-1168).

3.9 Mechanical properties and reliability

The advantages of centrifugal casting are obvious when comparing the mechanical properties, as shown in Fig. 18. These data were acquired from four-point-bending tests of batches of at least 21 specimens. The number of specimens is large enough to give good Weibull statistics.[35] The average strength of cast alumina was 540 MPa; an increase of 60% compared to isostatically pressed material (340 MPa). The Weibull modulus m of the centrifuged material was more than tripled, reaching 23·9. For the statistical calculation, the fracture probability estimator with the largest bias (mean rank value: $P_{if} = i/(n + 1)$) was chosen, leading to the lowest m-values of all known estimators.[36,37] These results prove that centrifugal casting provides the possibility of increasing the reliability of α-alumina ceramics up to the level requested by design engineers.

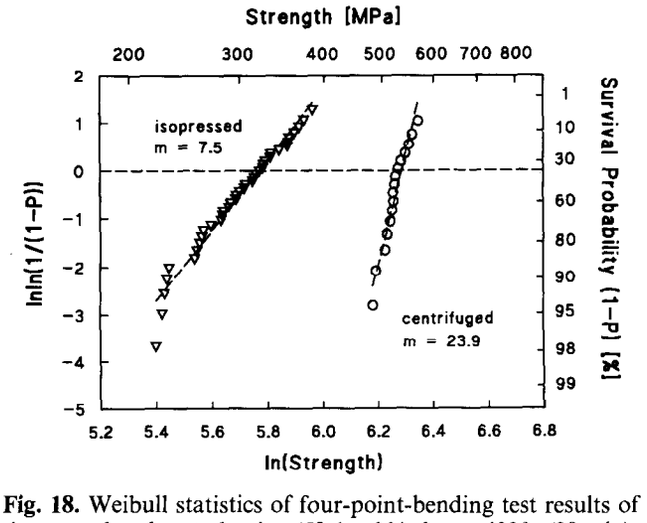

Fig. 18. Weibull statistics of four-point-bending test results of isopressed and cast alumina (53·4 vol.% slurry, 4000 *g*/90 min).

Table 3. Comparison of typical properties for cast and isostatic-pressed compacts

Property	*Centrifugal casting*	*Isostatic pressing*
Green density (%TD)	68	59
Sintered density (%TD)		
1400°C/6 h	99·4	98·6
1500°C/2 h	99·7	99·5
Linear shrinkage (%)	12	17
Average grain size (μm)	1·1	1·6
Maximum grain size (μm)	6	10
Maximum flaw size (μm)	20–30	90–120
Average strength (MPa)	540	340
Weibull modulus m	23·9	7·5

3.10 Comparison of centrifugal casting and isostatic pressing

In Table 3 some properties of compacts made via centrifugal casting and isostatic pressing are shown. The cast sample sinters to ≥99·4%TD at 1400°C with 6 h holding time, whereas the pressed sample requires a sintering temperature of 1500°C and 2 h to reach the same density. Centrifugal casting of high-solids-content slurries provides ceramic parts which have high green densities (15% higher than isopressed) and narrow pore size distributions and therefore closing of the structure is completed at lower temperatures and shrinkage is smaller. Higher green densities in combination with narrow pore size distributions leads to smaller grain sizes due to lower sintering temperatures. The largest flaws in the centrifuged parts are due to agglomerates not eliminated in the slurry preparation sequence. It can be expected that even better slurry preparation combined with smaller sieve size (from 1 to 5 μm) will reduce the maximum flaw size even more, leading to even higher strength values at higher reliabilities.

4 Summary and Outlook

α-Alumina ceramic components showing high reliability at high bend strength levels can be obtained from commercially available powders via centrifugal casting. Wet processing of ceramic powders and subsequent centrifugal casting of high-solids-content suspensions provides a route to producing parts that show better particle packing and a smaller number and size of flaws than dry processed components. High green and sintered densities as well as homogeneous microstructures were achieved by centrifugal casting α-alumina with a four-point-bend strength of 540 MPA and a reliability characterized by a Weibull modulus of m = 23·9 could be obtained. Centrifugal casting of high-solids-loading slurries is a very promising way to form highly reliable, high-strength ceramic parts using conventional powders. This forming method can be used to form complex shaped parts, even with undercuts.

These very encouraging results concerning shape capability, strength and reliability of α-alumina components clearly showed a promising direction, but still can be improved. Slurry preparation eliminating agglomerates smaller than 30 μm will further increase strength and reliability. Strength levels of up to 1 GPa, combined with reliabilities of m = 40 using conventional powders, seem possible.

Acknowledgements

This research was supported by the Swiss KWF organization under contract no. 2243.1. Thanks are due to Dr Rieger, METOXIT AG, for helpful discussions and his continuous interest.

References

1. Alford, N. McN., Birchall, J. D. & Kendall, K., Engineering ceramics — the process problem. *Mater. Sci. Technol.*, **2**(4) (1986) 329–36.
2. Birchall, J. D., High strength ceramics: problems and possiblities. *J. Phys. Chem. Solids*, **49**(8) (1988) 859–62.
3. Gauckler, L. J., Processing and properties of advanced ceramics. In *High-Tech Ceramics: Viewpoints and Perspectives*, ed. G. Kostorz. Academic Press, 1989, pp. 59–105.
4. Lange, F. F., Fabrication reliability of ceramics: controlling of flaw populations. *Mater. Res. Soc. Symp.*, **60** (1986) 143–52.
5. Ross, J. W., Miller, W. A. & Weatherly, G. C., Computer simulation of sintering in powder compacts. *Acta Metall.*, **30** (1982) 203–12.
6. Rhodes, W. H., Agglomerate and particle size effects on sintering yttria-stabilized zirconia. *J. Am. Ceram. Soc.*, **64**(1) (1981) 19–22.
7. Petzow, G. & Exner, H. E., Particle rearrangement in solid state sintering. *Z. Metall. K.*, **67** (1976) 611–17.
8. Exner, H. E. & Bross, P., Material transport, rate and stress distribution during grain boundary diffusion driven by surface tension. *Acta Metall.*, **27** (1978) 1007–12.
9. Barringer, E. A. & Bowen, H. K., Formation, packing, and sintering of monodispersed TiO_2 powders. *J. Am. Cer. Soc.*, **65**(12) (1982) C-199.
10. Occhionero, M. A., Influence of particle packing on microstructural development during sintering. Case Western Reserve University, PhD 8611452, 1986.
11. Kendall, K., Alford, N. McN. & Birchall, J. D., The strength of green bodies. *British Ceramic Proceedings, Special Ceram.*, **8**(37) (1986) 255–65.
12. Alford, N. McN., Birchall, J. D. & Kendall, K., High-strength ceramics through colloidal control to remove defects. *Nature*, **330**(5) (1987) 51–3.
13. Persson, M., In *Surfactant and Colloid Chemistry in Ceramic Processing*, eds R. J. Pugh & L. Bergström. Marcel Dekker Inc., New York, 1994, pp. 292–4.
14. Kendall, K., Alford, N. McN., Tan, S. R. & Birchall, J. D., Influence of toughness on Weibull modulus of ceramic bending strength. *J. Mater. Res.*, **1**(1) (1986) 120–3.
15. Pober, R. L., Product and process integration: the need for a ceramics manufacturing science. In *High-Tech Ceramics: Viewpoints and Perspectives*, ed. G. Kostorz. Academic Press, 1989, pp. 17–28.

16. Lange, F. F., Powder processing science and technology for increased reliability. *J. Am. Ceram. Soc.*, **72**(1) (1989) 3–15.
17. Buscall, R., The sedimentation of concentrated colloidal suspensions. *Colloids and Surfaces*, **43** (1990) 33–53.
18. Lange, F. F., Forming a ceramic by flocculation and centrifugal casting. US Patent 4 624 808, 25.11.1986.
19. Chang, J. C., Velamakanni, B. V., Chang, J. C., Lange, F. F. & Pearson, D. S., Centrifugal consolidation of Al_2O_3 and Al_2O_3/ZrO_2 composite slurries versus interparticle potentials: particle packing and mass segregation. *J. Am. Ceram. Soc.*, **74**(9) (1991) 2201–4.
20. Beylier, E., Pober, R. L. & Cima, M. J., Centrifugal casting of ceramic components. In *Ceramic Powder Science III, Ceramic Transactions*, **12**, eds G. L. Lessing, S. Hirano & H. Hausner. American Ceramic Society Inc., Westerville, Ohio, 1990, pp. 529–36.
21. Lange, F. F., Sinterability of agglomerated powders. *J. Am. Ceram. Soc.*, **67**(2) (1984) 83–9.
22. Salmovich, E. B. & Lange, F. F., Densification of large pores: I. Experiments. *J. Am. Ceram. Soc.*, **75**(9) (1992) 2498–508.
23. Shih, W. H., Kim, S. I., Shih, W. Y. & Aksay, I. A., Consolidation of colloidal suspensions. *Mater. Res. Soc. Symp.*, **180** (1980) 167–72.
24. Bergström, L., Schilling, C. H. & Aksay, I. A., Consolidation behavior of flocculated alumina suspensions. *J. Am. Ceram. Soc.*, **75**(12) (1992) 3305–14.
25. Shih, W. H., Shih, W. Y., Kim, S. I. & Aksay, I. A., Equilibrium-state density profiles of centrifuged cakes of flocculated suspensions. *Mater. Res. Soc. Symp.*, **289** (1993) 251–8.
26. Abel, J. S., Stangle, G. C., Schilling, C. H. & Aksay, I. A., Sedimentation in flocculating colloidal suspensions. *J. Mater. Res.*, **9**(2) (1994) 451–61.
27. Shih, W. H., Shih, W. Y., Kim, S. I. & Aksay, I. A., Equilibrium-state density profiles of centrifuged cakes. *J. Am. Ceram. Soc.*, **77**(2) (1994) 540–6.
28. Nagae, H., Ito, A. & Toriyama, M., Forming of ceramics by centrifugal casting. *Kinki Chem. Soc. Jpn Chem. Express*, **5**(3) (1990) 173–6.
29. Huisman, W., Graule, T. & Gauckler, L. J., High quality ceramics by centrifugal slip casting. *Third Euro-Ceramics*, **1** (1993) 537–42.
30. Huisman, W., Graule, T. & Gauckler, L. J., Centrifugal casting of zirconia (TZP). *J. Eur. Ceram. Soc.*, **13**(1) (1994) 33–9.
31. Hidber, P., Baader, F., Graule, T. & Gauckler, L. J., Sintering of wet milled centrifugal slip casting. *J. Eur. Ceram. Soc.*, **13**(4) (1994) 211–19.
32. Underwood, E. E., *Quantitative Stereology*. Addison-Wesley Publ. Co., Reading, Mass., 1970, pp. 24, 140.
33. Evans, A. G. & Charles, E. A., Fracture toughness determination by indentation. *J. Am. Ceram. Soc.*, **59**(7–8) (1976) 371–2.
34. Scherer, G. W., Theory of drying. *J. Am. Ceram. Soc.*, **73**(1) (1990) 3–14.
35. Balaba, W. M., Stevenson, L. T. & Wefers, K., Probability estimators for Weibull statistics of the failure strengths of brittle powder compacts. *J. Mater. Sci. Lett.*, **9** (1990) 648–9.
36. Bergmann, B., On the estimation of the Weibull modulus. *J. Mater. Sci. Lett.*, **3** (1984) 689–92.
37. Bergmann, B., On the variability of the fracture stress of brittle materials. *J. Mater. Sci. Lett.*, **4** (1985) 1143–6.